

MRI based Therapeutic Vectors

**SangBock Lee, V. R. Singh*

Received: 26 August 2019 / Accepted: 5 October 2019 / Published online: 30 December 2019

©The Author(s) 2019


Abstract- The development of simultaneous therapy and imaging systems (Theranostics) for micro RNA (miRNA) is demanded the clinical application of RNA interference (RNAi) in cancer treatment and immune therapy. In this paper, we report a pH-sensitive, magnetic nanoparticle-based miRNA delivery system that can enable the safe and effective delivery, imaging by high-resolution Magnetic Resonance Imaging (MRI) and therapeutic ability through regulating of tumor metastasis and immune evasion via miRNA34a. Cationic poly-L-lysine-graft (PL) with a reactive silane moiety was stably immobilized onto the surface of the assembled manganese ferrite nanoparticles (MFs) through an emulsion process, ensuring high water solubility, enhanced MR contrast effect, and endosome-disrupting functionality.

The MRI based theranostic nanovectors (MNVs) were then complexed with miRNA34a via electrostatic interaction to verify the regulation for cancer metastasis by CD44 and immune avoidance by regulating PD-L1. These results showed a novel platform for synergetic cancer therapy based on miRNA.

Key Word: miRNA34a, CD44, PD-L1, Cancer Treatment, Immune Evasion, MRI, Theranostics

I. Introduction

MicroRNAs (miRNAs)—small (20–22 nucleotide), endogenous, non-coding RNAs—act as regulators of gene expression at the post-transcriptional level through RNA interference. Mature miRNAs, which can regulate multiple target genes, associate with 3'-untranslated regions (3'-UTR) of specific target mRNAs to suppress translation and occasionally lead to their degradation. [1][2] Also, microRNAs (miRNAs) are actively involved in a variety of cellular processes, including differentiation, proliferation, and apoptosis. [3] Aberrant miRNA levels have an impact on many diseases, such as cancer, where miRNAs serve as both tumor suppressors and oncogenes. [3] In addition,

S.B. Lee 

**SangBock Lee*

Department of Radiology, Nambu University, 62271, Gwangju, Republic of Korea

**corresponding author*

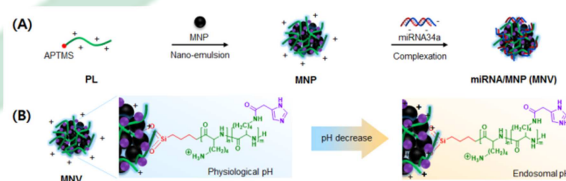
V. R. Singh

Director, PDM University, India

e-mail : vr-singh@ieee.org

Programmed death-ligand 1 (PD-L1) is a 40kDa type 1 transmembrane protein that has been considered to play a major role in suppressing the [immune system](#) during particular events such as pregnancy, tissue [allografts](#), autoimmune disease and other disease states such as hepatitis, it may allow cancers to evade the host immune system. [4][5] An analysis of 196 tumor specimens from patients with [renal cell carcinoma](#) found that high tumor expression of PD-L1 was associated with increased tumor aggressiveness and a 4.5-fold increased risk of death. [6] Consequently, tumor can exploit the PD-L1 pathway to inhibit the anti-tumor immune response. [7] Recently, PD-L1 which plays an important role in the antitumor effect, has been studied in the world, especially, research in the miRNA-mediated regulation of PD-L1 has been widely progressed. [7] It had previously demonstrated that miR-200 inhibited PD-L1, explaining how prevented epithelial-to-mesenchymal transition and metastasis in lung cancer, Welsh et al have investigated the role of miR34a in regulating PD-L1 activity, also, miRNA34a modulates PD-L1 to induce immune evasion, as well as to regulate cancer metastasis by regulating CD44, an important marker of cancer. [8][9] However, it is big issue for delivering miRNA, in order to safely deliver of Gene such as miRNA in vivo, appropriate delivery systems are also required for efficient and safe delivery of miRNAs. Recent research have evaluated many nonviral vectors incorporating imaging agents (i.e., magnetic nanoparticles, gold nanoparticles and fluorescence molecules) as promising carriers for simultaneous imaging and gene delivery. [10][11] These research have shown that such vectors can improve therapeutic efficacy and tumor accumulation through real-time monitoring of the miRNA-delivery process, for the clinical applicability of miRNA-mediated

therapy, simultaneous imaging and gene delivery is important to improve therapeutic efficacy, bio-distribution, and tumor accumulation of nanovectors by facilitating visualization of the miRNA delivery process. For this purpose, a number of inorganic formulations (i.e., magnetic nanoparticles, gold nanoparticles, and quantum dots, etc.) are being evaluated as attractive materials for miRNA delivery and imaging due to their special properties such as facile surface modification, size control, and imaging modalities. Among them, magnetic nanoparticles (MNPs) enable the monitoring of miRNA delivery by non-invasive and real-time magnetic resonance imaging (MRI), because this technique can rapidly acquire multi-informational high resolution images. To accomplish this, miRNAs need to be reversibly packed into MNPs allowing them to be transported into the cytoplasm and carry out the RNAi functional mechanism effectively. Several approaches can be implemented to introduce miRNA into MNPs, including cleavable linkers, electrostatic interactions, or incorporation into polymeric matrix composites. For the safe and effective intracellular delivery of miRNA with MR contrast agents, the nanoplatform should 1) be sufficiently cationic to condense miRNA, 2) have no significant inhibition of growth and proliferation on cells, 3) be promptly



Scheme. (A) Schematic illustration of the synthesis of pH-sensitive magnetic nanovectors (MNV) with and magnetic nanoparticles (MNPs) through the emulsion process, and the formation of MNV/miRNA34a complexes *via* electrostatic interaction. (B) Schematic illustration of a rapid

change in the surface charge of MNV in response to a reduction in pH as a result of pH-activated protonation.

disassembled under pH reduction to lead endosomal escape, and 4) have ultrasensitive magnetic properties after uptake. Herein, we developed magnetic nanovectors (MNVs) by the emulsion and solvent evaporation method using pH-sensitive polycations that stabilize and envelop MNPs in Schematic image, and demonstrated their utility for cancer detection by MRI and synchronous delivery of therapeutic miRNA. For the complexation of miRNA and to provide a buffering effect under acidic pH, the hydrophilic and cationic homopolymer poly-L-lysine (PL) with a silane terminal group was first prepared by consecutive processes of ring-opening polymerization and deprotection. The obtained PL was used not only for the self-assembly of the manganese ferrite (MnFe_2O_4) nanoparticles (MFs) but also for gene loading at the outer layer of MFs, finally producing water-dispersible, magnetic particles core-polycation shell nanostructures. These results demonstrate that magnetic nanovectors have potential as theragnostic nanosystems for regulating immune evasion and tumor metastasis based on miRNA in effective cancer therapy.

II. Materials and Methods

A. Materials

N^6 -carbobenzyloxy-L-lysine (LysZ), 4-imidazoleacetic acid, (3-aminopropyl) trimethoxysilane (APTMS), 1-ethyl-3-(3-dimethylaminopropyl) carbodiimide (EDC) hydrochloride, trifluoroacetic acid (TFA), hydrobromic acid solution (33 wt % in acetic acid) (HBr/AcOH), anhydrous tetrahydrofuran (THF),

N,N -dimethylformamide (DMF), dimethylsulfoxide (DMSO), 1N sodium hydroxide (NaOH) solution, iron (III) acetylacetonate, manganese (II) acetylacetonate, 1,2-hexadecanediol, lauric acid, lauryl amine, benzyl ether, deuterium oxide (D_2O), and dimethylsulfoxide- d_6 (DMSO- d_6) were purchased from Sigma-Aldrich (St. Louis, MO, USA). Triphosgene was acquired from Tokyo Chemical Industry Co. (Tokyo, Japan), and 1-hydroxybenzotriazole hydrate (HOBt) was obtained from Daejung Chemicals & Metals Co. (Shiheng, Korea). n-Hexane and diethyl ether were obtained from Ducksan Scientific Co. (Seoul, Korea) The miRNA34a (miR34a) (Sense : ACA ACC AGC UAA GAC ACU GCC A/iSp9//3ThioMC3-D, antisense : UGG CAG UGU CUU AGC UGG UUG U) was purchased from Messenger of Biotechnology Co. (Gyeonggi, Korea), and the hydroxyl PEG Thiol was purchased Nanocs.

B. Methods

1. Synthesis of N^6 -carbobenzyloxy-L-lysine N-carboxyanhydride (LysZ-NCA)

Synthesis of N-carboxyanhydride of L-lysine was conveyed out by the Fuchs-Farthing method using triphosgene. To make ready N^6 -carbobenzyloxy-L-lysine (LysZ) N-carboxyanhydride (LysZ-NCA), LysZ (2 g, 7.13 mmol) was suspended in 145 mL of anhydrous THF. Triphosgene (0.85 g, 2.85 mmol) solution dissolved in 5 mL of THF was injected into the LysZ-suspended solution using a syringe under nitrogen atmosphere. The reaction was performed at 35°C for 3 hr under magnetic stirring, and the appearance of the reactant solution changed from cloudy to clear after all LysZ molecules were transformed into LysZ-NCA. The solvent was filtered through a $0.2\text{-}\mu\text{m}$ PTFE syringe filter

(Advantec MFS, Inc., Japan) to remove impurities, followed by evaporation of the filtrate under the reduced pressure. The concentrated reactants were introduced to cold excess n-hexane, and the n-hexane/THF mixture was then recrystallized at -20°C overnight. The precipitants were purified three times by filtration and dried at room temperature *in vacuo*. Yield: 70%. FT-IR (cm⁻¹): ν = 3340 (s, NH), 3070-2870 (s, CH₂), 1855/1810/1774 (s, C=O in anhydrides of NCA), 1745 (s, C=O in Z group), 1685 (s, C=O in amide of NCA) 1528 (s, NH in amide of NCA). ¹H-NMR (400 MHz, DMSO-d₆, ppm): δ = 9.09 (w, α -NH), 7.54-7.26 (s, Ar-H in benzyl groups), 5.04-5.00 (s, -CH₂ in benzyl groups), 4.44-4.41 (w, α -CH), 3.01-2.96 (m, ϵ -CH₂), 1.72-1.30 (m, γ -CH₂ and δ -CH₂).

2. Synthesis of APTMS-initiated poly-L-lysine (PL) by ring opening polymerization

To synthesize poly (N⁶-carbobenzyloxy-L-lysine) (PLZ), the polymerization of LysZ-NCA initiated by APTMS proceeded as follows. Briefly, LysZ-NCA (10 g, 32.65 mmol) was dissolved in 50 mL of anhydrous DMF. APTMS (73.16 mg, 0.41 mmol) was injected into the solution as an initiator using a syringe under a blanket of nitrogen, and the mixture was reacted at 40°C for 24 hr. The solvent was evaporated under reduced pressure and precipitated in excess cold diethyl ether. The purified precipitates were isolated by repeated filtration and dried under high vacuum. Yield: 61.11%. FT-IR (cm⁻¹): ν = 3198 (s, NH), 3062-2866 (s, CH₂), 1693 (s, C=O in Z group), 1653 (s, C=O in amide), 1530 (s, NH in amide). ¹H-NMR (400 MHz, DMSO-d₆, ppm): δ = 8.44-7.88 (w, α -NH), 7.53-7.19 (s, Ar-H in benzyl groups), 4.99 (s, -CH₂ in benzyl groups), 4.31-4.11 (w, α -CH), 2.95 (m, ϵ -CH₂), 1.62-1.27 (m, γ -CH₂ and δ -CH₂). The obtained PLZ was further

characterized by gel permeation chromatography (YL9100 HPLC, Young Lin Instrument Co., Ltd., Korea) equipped with two Waters styragel HR3 columns (Waters Co., Milford, MA) and a refractive index detector through HPLC-grade DMF at 1.0 mL/min. The molecular weight distribution (M_w/M_n) of the polymer was determined to be 1.2. To remove the Z protection groups, PLZ (7 g, 0.33 mmol) was dissolved in 70 mL of TFA and then 10 mL of HBr/AcOH was added to the mixture. The mixture was gently stirred at room temperature for 1.5 hr and the resulting product was isolated three times by filtration with excess diethyl ether. The polymer was further dialyzed against multiple ultrapure distilled water.

3. Fabrication of PL-coated magnetic nanoparticles

Magnetic Nanovectors (MNVs) as gene loadable MR imaging agents were prepared by the nano-emulsion method. Firstly, monodisperse manganese ferrite (MnFe₂O₄) nanoparticles (MFs) were synthesized by the thermal decomposition of metal-organic precursors in the presence of nonpolar organic solvents. In detail, iron (III) acetylacetonate (2 mmol), manganese (II) acetylacetonate (1 mmol), 1,2-hexadecanediol (10 mmol), lauric acid (6 mmol), and laurylamine (6 mmol) were dissolved in 20 mL of benzyl ether. The solution was preheated to 200°C for 2 hr under an ambient nitrogen atmosphere and refluxed at 300°C for 1 hr. After cooling the reactants to room temperature, the products were purified using an excess of pure ethanol. Approximately 11-nm MFs were synthesized using the seed-mediated growth method. Twenty milligrams of the as-synthesized MFs were dissolved in 4 mL of n-hexane and subsequently added into 20 mL of DW containing 50, 100, or 200 mg of PL. After mutual

saturation of the organic and aqueous phases, the mixture was ultrasonicated at 200 W for 20 min with vigorous stirring at 1,500 rpm, and stirred for 4 hr to evaporate the residual hexane.

4. Preparation of miRNA loaded magnetic nanoparticles

The miRNA condensation ability of MNPs was confirmed by the gel retardation assay. To compare miRNA-loading ability, miRNA was also complexed with varying amounts of MNPs. The prepared complexes were mixed with 6x HiQ™ goRed (Genepole, Seoul, Korea), then loaded into a 2% agarose gel (w/v), and electrophoresed in Tris – borate – EDTA (TBE) buffer at 100 V for 20 min. The retardation of complexes was visualized by a UV lamp using a Gel Doc System.

III. Experiments.

1. Characterizations of magnetic nanovectors

The average hydrodynamic diameters and zeta potentials of the obtained magnetic Nanovectors (MNVs) were measured using dynamic laser scattering at room temperature. Their size distributions and morphologies were observed by transmission electron microscopy at an accelerating voltage of 200 kV. The concentration of Mn plus Fe ions in the MNVs was measured by using inductively coupled plasma-atomic emission spectrometry (ICP-AES) analysis. The magnetic hysteresis loop and the saturated magnetization value were obtained using a vibrating sample magnetometer at 25°C. The amount of MFs encapsulated in MNVs was measured by thermal gravimetric analysis. The T2 relaxivity (r_2) data of the MNV solution were obtained through

magnetic resonance (MR) imaging analysis.

2. Cell viability test

The cytotoxicity of MNVs in gastric cancer MDA-MB-231 cells was evaluated by a colorimetric assay, based on the cellular reduction of 3-(4,5-dimethylthiazoly-2)-2,5-diphenyltetrazolium bromide (MTT) (Cell Proliferation Kit I, Roche, Germany) in metabolically active cells. MDA-MB-231 cells (1×10^4 cells/well) were seeded into 96-microwell plates, incubated in RPMI 1640 medium containing 5% fetal bovine serum (FBS) and 1% antibiotics at 37°C overnight in a humidified atmosphere with 5% CO₂, and then treated with MNVs containing medium with 5% FBS at various concentrations for additional 24 hr. After incubation, the yellow MTT solution was added and the formazan crystals formed were solubilized with 10% sodium dodecyl sulfate in 0.01 M HCl. Then the relative percentage of cell viability was calculated from the formazan intensity ratio of treated to non-treated control cells and shown as an average \pm standard deviation.

3. MR imaging procedures

We performed solution and in vitro, in vivo MR imaging experiments with a 4.7 T clinical MRI instrument. The R2 values (T2 relaxation rate, $1/T_2$, s^{-1}) of the MNV solution and miR34a-MNP treated cells (1×10^7) were measured by using the conventional T2 sequence at room temperature. For the acquisition of T2 weight MR images of MNV solution, MNV treated cells and in vivo MR imaging the following parameters were adopted : resolution of xxx x xxx mm, section thickness of x mm TE = x ms, TR = x ms, and number of acquisitions = 1, The r_2 ($Mm^{-1}s^{-1}$) is equal to the ration of the R2 to the MNV concentration.

4. Cellular uptake of MNVs

To prepare cellular TEM samples, MDA-MB-231 cells (1×10^6) were harvested after TrypLE™ (Gibco®) treatment, washed in triplicate with blocking buffer (0.03% bovine serum albumin and 0.01% NaN_3 in phosphate-buffered solution, pH 7.4 and 10 mM) to prevent non-specific binding, and gently pelleted. Subsequently, the cells were suspended in MNV solution (0.46 $\mu\text{g}/\text{mL}$) and incubated for 30 min on ice and 30 min at 37°C. After incubation, the cells were washed three times with blocking buffer and fixed according to the standard fixation and embedding protocol for resin-section TEM. The sample resin blocks were trimmed and sectioned using a LEICA Ultracut UCT Ultramicrotome (Leica Microsystems Ltd., Austria). Cellular uptake of MNVs was also examined by the Prussian blue staining method. To stain magnetic components in MDA-MB-231 cells treated with MNVs (0.46 $\mu\text{g}/\text{mL}$), the cells were incubated with 2% potassium ferrocyanide in 10% HCl and then counterstained with Nuclear Fast Red (Sigma-Aldrich). Cellular internalization of the MNVs was observed by TEM at an accelerating voltage of 80 kV and an epi-fluorescence microscope.

IV. Result & discussion

1. In vitro transfection and quantitative reverse transcriptase-polymerase chain reaction (qRT-PCR) analysis

To measure CD44, PDL1 mRNA expression levels in cancer cells, real time qRT-PCR analysis with internal standards was performed. Firstly, MDA-MB-231 cells (2×10^5 cells/well) were seeded in six-well plates containing 2 mL culture medium supplemented with 5 % FBS and incubated at 37°C overnight to reach 70% confluence at the time of

transfection. The culture medium was then replaced with serum-free medium and 100 μL of MNPs containing miR34a or control miR34a (100 pmol) at a polycation/miRNA weight ratio of 1:2 was added to each well. As a control, MDA-MB-231 cells were also transfected with free miR34a or control miR34a. After 6 hr incubation, the medium was replaced with 2 mL fresh culture medium and further incubated at 37°C for 48 hr. The cells were harvested 48 hr after transfection, and total RNA was isolated from the cells with the RNeasy® Plus Mini Kit (QIAGEN, Hilden, Germany), according to the manufacturer's instructions. Complementary DNA (cDNA) was synthesized from 2 μg of total RNA using the High Capacity RNA-to-cDNA kit (Applied Biosystems®). The resulting cDNA was amplified by PCR, conducted with the QuantiMix SYBR Kit (PhileKorea Technology, Daejeon, Korea) on a real-time PCR system (LightCycler® 480 System, Roche). Primer sequences were as follows: CD44, forward 5'-CCTCTT GGCCTTGGCTTTG-3' and reverse 5'-TCCATTGCCACTGTTGATCA-3'; PD-L1, forward 5'-AAATGGAACCTGGCGAAAGC-3' and reverse 5'-GATGAGCCCCTCAGGCATTT; GAPDH, forward 5'-GCTCTCTGCTCCTCCTGTTC-3' and reverse 5'-TGACTC CGACCTTCACCTTC-3'. The PCR conditions were as follow: initial denaturation at 95°C for 10 min; 45 cycles of amplification at 95°C for 10 sec, at 60°C for 10 sec, and at 72°C for 10 sec. Each sample was performed in triplicate. The relative CD44 mRNA expression value was normalized to the endogenous reference gene (GAPDH) in the corresponding samples and relative to non-treated cells, and calculated by the $\Delta\Delta\text{C}_t$ method.

2. In vitro Western blot analysis

To assess the down-regulation of the CD44, PD-

L1 gene in MDA-MB-231 cells, the cells were harvested and lysed in cold RIPA buffer (Pierce[®], Thermo Scientific) containing a protease inhibitor cocktail tablet (complete Mini, Roche). The lysates were incubated at 4°C for 30 min and centrifuged at 13,000 rpm for 15 min. The supernatants were analysed for protein concentrations using the bicinchoninic acid (BCA) Protein Assay (Pierce[®]). Equal amounts (20 µg) of protein were subjected to electrophoresis on sodium dodecyl sulfate (SDS)-polyacrylamide gels and then transferred to a nitrocellulose blotting membrane (Amersham™ Hybond ECL, GE Healthcare). The blotted membranes were immunostained with antibodies specific for CD44 (156-3C11, Cell Signalling Technology, Inc., USA), PD-L1 (22C3, Dako, Inc, USA) and GAPDH antigens (6C5, Santa Cruz Biotechnology, Inc., USA). The signals were developed by a standard enhanced chemiluminescence (ECL) method (Pierce[®] ECL Plus Western Blotting Substrate) according to the manufacture's protocol.

3. Wound healing assay

For the evaluation of the migration and mobility of MDA-MB-231 cells treated with MNVs, the wound healing assay was carried out. The cells were transfected with nanovector formulations with miR-34a or control miR and grown to 100% confluence in culture media. Using a sterile pipette tip, the cell monolayer was mechanically scratched inducing the wound and further incubated with culture media for 4 days. The

images of the wound closing were captured with an inverted microscope.

4. Invasion assay analysis

At first, to lay HUVEC cells, Coat the inside of transwell with 50µL Fibronectin (10 µg/mL) at the bottom and dry for 2-3 hours at RT. Coat the bottom of transwell with 10µL of 0.2% gelatin and dry for 30 min at RT. After that add 2×10^4 endothelial cells (HUVEC) in 50µL of culture medium (M199) to insert. And culture the cells for 48 hours until forming monolayer. At seconds, in order to stain the cells, when the cells reached 70% confluence remove the medium from the dish. And add fresh medium (0% FBS) with Cell tracker dye (0.5µM) Incubate the cells for 1hours. Replace the dye working solution with culture medium (10% FBS) for 30min. To lay tumor cells which treated cell tracker, harvest tumor cells with 0% culture medium, and add $1 \times 10^5/50 \mu\text{L}$ tumor cells to insert. And add 605 µL with culture medium (10% FBS) to the lower chamber. Incubate the cells for 48 hours. To measure cell which passing the MEM, remove the upper cells of membrane by cotton swab. Lysis the cells on lower membrane with 200 µL lysis buffer, 2-3 hours at RT. Read absorbance (Abs/Em : 492/517)

5. In vivo tumor growth inhibition, target gene silencing and immune evasion

For the inhibition study of tumor growth using MNVs, here we used a subcutaneous xenograft

tumor model that allows routine and facile measurements of tumor volume. A cancer model was established by subcutaneously injecting MDA-MB-231 cells (10^7 cells suspended in 50 mL of PBS per animal) into the breast of the BALB/c-nude mice. Tumor bearing mice were randomized into 3 different groups for treatments (non-treated, control miRNA34a/MNV treated groups and miR-34a/MNV-treated groups), when the tumor volume increased to 200 mm^3 . Prior to administration of each formulation, animals were anesthetized and injected with control miRNA34a/MNV and miR-34a/MNV (1 nmole of miR-34a per injection) through the tail vein twice per week for 3 weeks. The tumor volume was calculated using the formula: $V = \frac{1}{4} \left(\frac{4}{3} \pi a^2 b \right)^2$, where a and b are the half length of the minor and major axis of tumors determined by a caliper. All mice were sacrificed after 7 weeks post-treatment and the extracted tumor tissues were used for H&E staining, TUNEL assay. The tumor sections were then counterstained with Hoechst 33342 and PE mouse anti-human CD44 (BD Pharmingen, Cat. No. 550989), PD-L1 (Dako, Cat. No. 22C3). The expression levels of CD44, PD-L1 in the excised tumor tissues after crushing in liquid nitrogen were also verified by western blot assay using the same procedures as described in in vitro analysis

V. Conclusion

We present the pH-sensitive, magnetic nanoparticle-based miRNA delivery system that can facilitate the safe and efficient delivery,

imaging by high resolution MRI and therapeutic ability through regulating of tumor metastasis and immune evasion via miRNA34a. Cationic poly-L-lysine-*graft* (PL) with a reactive silane moiety was stably immobilized onto the surface of the assembled manganese ferrite nanoparticles (MFs) through an emulsion process, ensuring high water solubility, enhanced MR contrast effect, and endosome-disrupting functionality. We verified the in vivo and in vitro specific CD44 gene knockdown effects of MNVs in MDA-MB-231 cells using both qPCR and Western blot analysis. We found that the regulation through miR34a enable to cancer metastasis by CD44 and immune avoidance by regulating PD-L1. Consequently, we designed theranostic system would be beneficial to expand research on miRNA based and immune therapy for cancer.

Competing interests

The authors declare that there is no conflict of interest regarding the publication of this paper.

Acknowledgments

This study was supported by Nambu University research fund of 2017.

[References]

1. Minju Ha, V. Narry Kim, "*Regulation of microRNA*", Nature Reviews Molecular Cell Biology 2014, **15**:509-524.
2. Lin He, Gregory J Hannon, "*MicroRNAs: small RNAs with a big role in gene regulation*", Nature Review Genetics 2004, **5**:631.

3. George A. Calin, Carlo M. Croce, "***MicroRNA signatures in human cancers***", Nature Review Genetics 2006, **6**: 857-866
4. Keisuke Kataoka¹, Yuichi Shiraishi, et al, "***Aberrant PD-L1 expression through 3'-UTR disruption in multiple cancers***", Nature 2016, **534** : 402-406
5. Diana Romero, "***Benefit with anti-PD-L1***", Nature Reviews Clinical Oncology 2017, **14** : 70-71
6. Thompson RH, Gillett MD, Cheville JC, Lohse CM, et al, "***Costimulatory B7-H1 in renal cell carcinoma patients: Indicator of tumor aggressiveness and potential therapeutic target***", Proceedings of the National Academy of Sciences of the United States of America 2004, **101** : 17174-9
7. Jiabei He, Ying Hu, Mingming Hu, Baolan Li, "***Development of PD-1/PD-L1 Pathway in Tumor Immune Microenvironment and Treatment for Non-Small Cell Lung Cancer***", Scientific Reports 2015, **5** : 13110
8. Maria Angelica Cortez, Cristina Ivan, David Valdecanas, et al, "***PDL1 Regulation by p53 via miR-34***", Journal of National Cancer Institute 2016, **108** : 303
9. Can Liu¹, Kevin Kelnar, Bigang Liu, Xin Chen¹, et al, "***The microRNA miR-34a inhibits prostate cancer stem cells and metastasis by directly repressing CD44***", Nature medicine 2011, **17** : 211-215
10. Jae-Hyun Lee, Kyuri Lee, Seung Ho Moon, Yuhan Lee, Tae Gwan Park, and Jinwoo Cheon, "***All-in-One Target-Cell-Specific Magnetic Nanoparticles for Simultaneous Molecular Imaging and siRNA Delivery***", Angewandte Chemie International Edition 2009, **48** : 4174-4179
11. Huan Meng, Monty Liong, Tian Xia, Zongxi Li, et al, "***Engineered Design of Mesoporous Silica Nanoparticles to Deliver Doxorubicin and Pgp siRNA to overcome Drug Resistance in a Cancer Cell Line***", ACS Nano 2010, **24** : 4539-4550